Case Report | Nuclear Medicine

http://dx.doi.org/10.3348/kjr.2014.15.1.169
pISSN 1229-6929 · eISSN 2005-8330
Korean J Radiol 2014;15(1):169-172

Korean Journal of Radiology
KJR

Von Hippel-Lindau Syndrome: Demonstration of Entire Disease Spectrum with ^{68}Ga-DOTANOC PET-CT

Punit Sharma, MD, Varun Singh Dhull, MD, Chandrasekhar Bal, MD, Arun Malhotra, PhD, Rakesh Kumar, MD, PhD

All authors: Department of Nuclear Medicine, All India Institute of Medical Sciences, New Delhi 110029, India

Von Hippel-Lindau (VHL) syndrome is a rare neoplastic disorder characterized by central nervous system (CNS) and visceral tumors. We here present ^{68}Ga-labelled [1, 4, 7, 10-tetraazacyclododecane-1, 4, 7, 10-tetraacetic acid]-1-Nal3-Octreotide positron emission tomography computed tomography findings in a 52 year old female with VHL syndrome, demonstrating both CNS and visceral tumors.

Index terms: *Von Hippel-Lindau syndrome; ^{68}Ga-DOTANOC; PET-CT; Hemangioblastoma; RCC; NET*

INTRODUCTION

Von Hippel-Lindau (VHL) syndrome is an autosomal dominant neoplastic disorder. It is commonly characterised by retinal and central nervous system (CNS) hemangioblastomas, clear cell renal cell carcinoma (RCC), pheochromocytoma, pancreatic islet tumors and endolymphatic sac tumors (1). Diagnosis is generally clinical, although specific gene mutation can be demonstrated (2). Imaging plays an important role in diagnosis. ^{68}Ga-labelled [1, 4, 7, 10-tetraazacyclododecane-1, 4, 7, 10-tetraacetic acid]-1-Nal3-Octreotide (^{68}Ga-DOTANOC) positron emission tomography computed tomography (PET-CT) is now being routinely employed for somatostatin receptor (SSTR), based PET imaging at many centers. It binds to the cell membrane SSTR receptors (subtype 2, 3 and 5) and can be employed for high resolution PET imaging. ^{68}Ga-DOTANOC PET-CT has proven to be very useful for imaging of neuroendocrine tumors (NET). We here present a case of a 52 year old lady with VHL syndrome, where ^{68}Ga-DOTANOC PET-CT demonstrated both CNS and visceral tumors.

Received July 25, 2012; accepted after revision September 20, 2012.
Corresponding author: Punit Sharma, MD, Department of Nuclear Medicine, All India Institute of Medical Sciences, New Delhi 110029, India.
• Tel: (9111) 26593210 • Fax: (9111) 26588663
• E-mail: dr_punitsharma@yahoo.com

CASE REPORT

A 52-year-old lady remove was presented with an abdominal lump of 6-month in duration. She gave history of left eye surgery five years back, following an episode of sudden onset loss of vision. Since then, she had loss of vision in the left eye. There were no other CNS symptoms. She also gave history of similar eye surgery in her younger son (age-28 years), following a similar episode of unilateral loss of vision. On examination, she was not hypertensive. She had no perception of light in the left eye, while the right eye visual acuity was normal. Because of the presence of secondary cataract in the left eye, her posterior chamber could not be evaluated. There were no cerebellar signs. Abdominal examination revealed a large lump in the right upper and lower quadrant. Complete hemogram, renal function tests and liver function tests were normal.

Contrast enhanced CT of the abdomen revealed a

hypervascular mass (7.8 x 5.8 x 5.1 cm), arising from the interpolar region of the left kidney with multiple feeding vessels arising from the left renal artery and supplying the mass (Fig. 1A, D). The findings were suspicious for RCC. Multiple cortical cysts were also seen in both kidneys. Another large (9.6 x 7.4 x 5.4 cm) hypervascular mass lesion was seen in the body and tail of the pancreas, which was suspicious for metastasis from RCC (Fig. 1A). Bilateral adrenals were normal. Because of the hypervascular nature of pancreatic mass biopsy was not attempted.

Subsequently, SSTR PET-CT was done with ^{68}Ga-DOTANOC to characterize the pancreatic mass. PET-CT revealed intense ^{68}Ga-DOTANOC uptake (maximum standardised uptake value [SUV_{max}] = 18.6) in the pancreatic mass, characterizing it as a NET (Fig. 1B, C). It also demonstrated a solitary liver metastasis (segment III) with intense ^{68}Ga-DOTANOC uptake (SUV_{max} = 13.2), confirming it to arising from pancreatic NET (Fig. 1B, C). The left renal mass showed only a mild ^{68}Ga-DOTANOC uptake (SUV_{max} = 3.1) (Fig. 1E, F). Interestingly, a hypodense lesion was seen in the left cerebellum, showing increased ^{68}Ga-DOTANOC uptake (SUV_{max} = 9.9) (Fig. 1G, H). Another focus of ^{68}Ga-DOTANOC uptake was seen in a lateral part of the left globe (SUV_{max} = 8.3) corresponding to a heterogeneous lesion seen on CT (Fig. 1J, K).

Gadolinium enhanced magnetic resonance imaging (MRI) of the brain was done to characterise the CNS lesions seen on ^{68}Ga-DOTANOC PET-CT. It showed a nodular lesion (2 x 2 cm) in the lateral half of the left cerebellar hemisphere with intense post contrast enhancement (Fig. 1I). An eccentric nodule was also noted in the lateral part of the left globe with intense post contrast enhancement (Fig. 1L). MRI findings were consistent with hemangioblastoma of the left retina and cerebellum. Imaging findings confirmed the diagnosis of VHL syndrome. Therefore, serum and

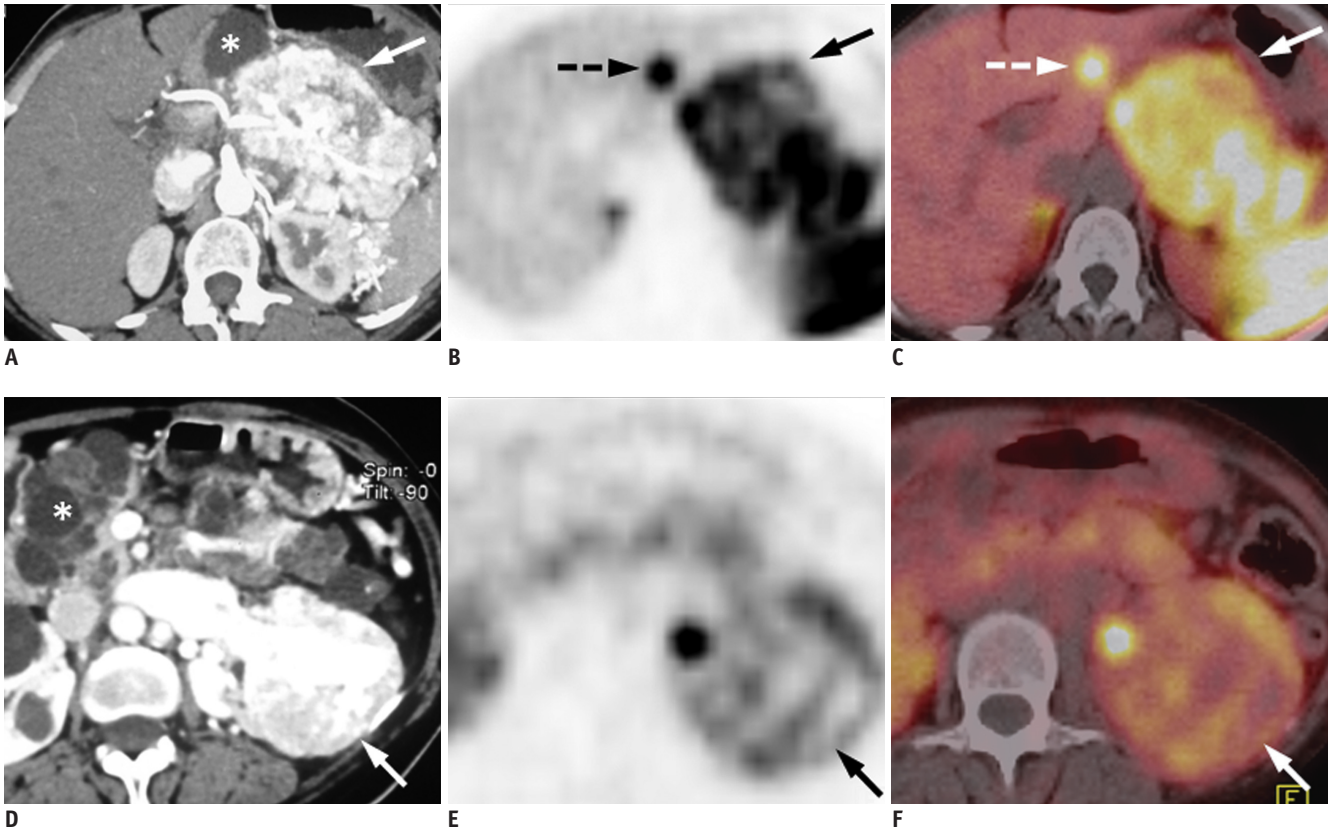

Fig. 1. 52-year-old female with Von Hippel-Lindau syndrome.
Transaxial contrast enhanced CT **(A)** of abdomen show large (9.6 x 7.4 x 5.4 cm) mass lesion in region of body and tail of pancreas with intense post contrast enhancement (arrow). Multiple cysts of varying sizes are noted in rest of pancreas (asterix). Also, note tortuous blood vessels in peripancreatic and perisplenic location. Transaxial PET **(B)** and PET-CT **(C)** images show intense heterogeneous uptake of ^{68}Ga-labelled [1, 4, 7, 10-tetraazacyclododecane-1, 4, 7, 10-tetraacetic acid]-1-Nal3-Octreotide (^{68}Ga-DOTANOC) (SUV_{max} = 18.6) in pancreatic mass (arrow), thus confirming it to be NET. Focal ^{68}Ga-DOTANOC uptake (SUV_{max} = 13.2) was also seen in segment III of liver (**B, C,** broken arrow) suggesting liver metastasis from pancreatic NET. This was confirmed at fine needle aspiration cytology. Transaxial contrast enhanced CT **(D)** of abdomen also shows another mass (7.8 x 5.8 x 5.1 cm) arising from interpolar region of left kidney and showing intense post contrast enhancement (arrow). Multiple feeding vessels are seen to arise from left renal artery and supply mass. These findings were suggestive of RCC. Also noted are bilateral multiple renal cortical cysts (asterix). PET **(E)** and PET-CT **(F)** images reveal mild ^{68}Ga-DOTANOC uptake (SUV_{max} = 3.1) in renal mass (arrow).

Korean Journal of Radiology
KJR

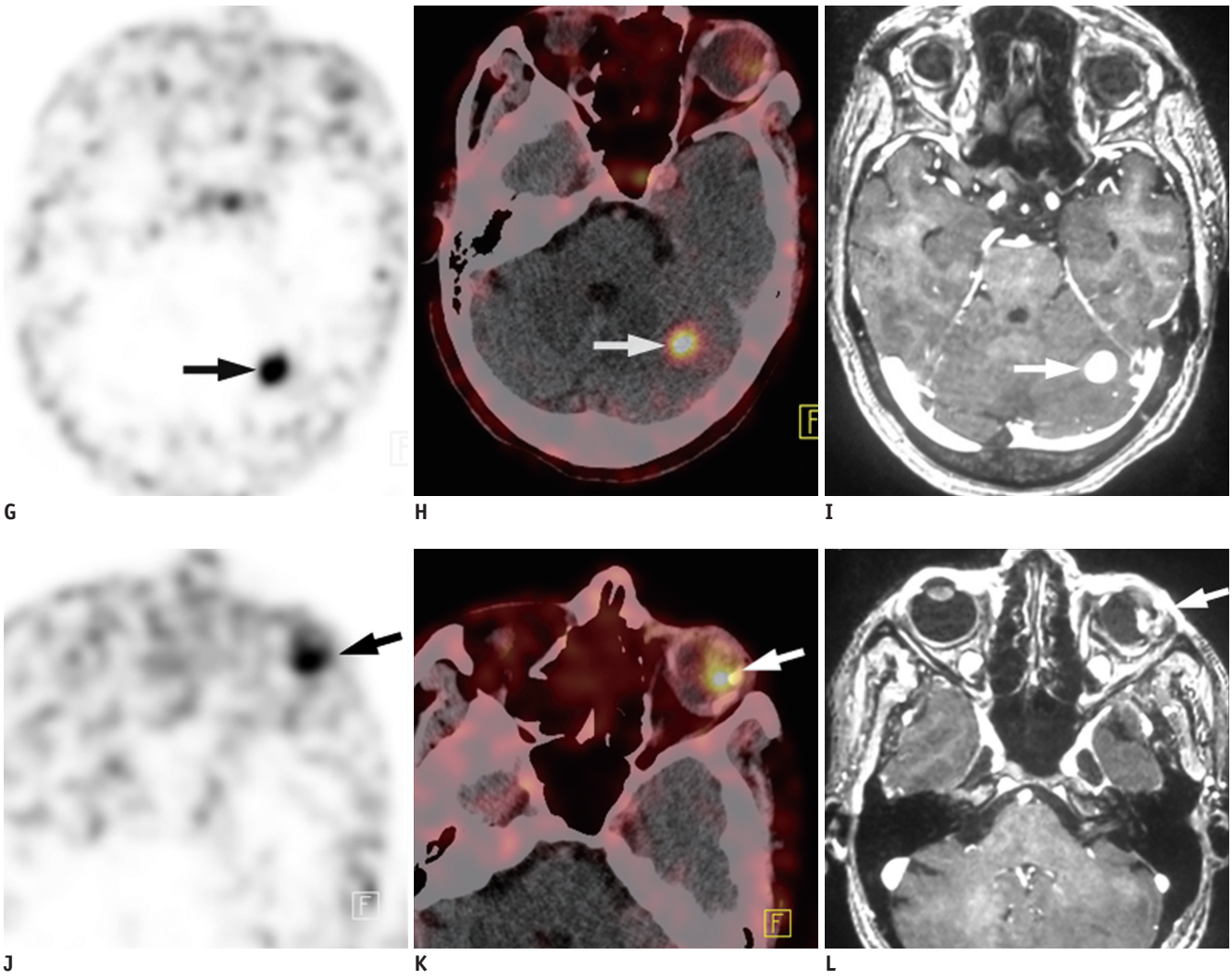

Fig. 1. 52-year-old female with Von Hippel-Lindau syndrome.
Transaxial PET **(G)** and PET-CT **(H)** images of brain show focal area of ^{68}Ga-DOTANOC uptake (SUV_{max} = 9.9) in hypodense lesion (2 x 2 cm) in left cerebellum (arrow). Transaxial T2 weighted gadolinium enhanced MRI **(I)** of brain reveals nodular lesion in lateral half of left cerebellar hemisphere with intense post contrast enhancement (arrow), suggesting hemangioblastoma. Transaxial PET **(J)** and PET-CT **(K)** images also revealed focal ^{68}Ga-DOTANOC uptake (SUV_{max} = 8.3) in lateral part of left globe, corresponding to heterogeneous nodular lesion (arrow). Transaxial T2 weighted gadolinium enhanced MRI **(L)** showed eccentric nodule in lateral part of left globe with intense post contrast enhancement, suggesting retinal hemangioblastoma (arrow).

urinary catecholamines levels were done for screening of pheochromocytoma and paraganglioma, and were found to be normal. Fine needle aspiration cytology from the liver lesion confirmed the diagnosis of metastatic NET. The patient is now being worked up for palliative radionuclide therapy with ^{177}Lu-DOTATATE.

DISCUSSION

Von Hippel-Lindau syndrome is an autosomal dominantly inherited neoplastic disorder that demonstrates age-dependent penetrance and marked phenotypic variability. The basic underlying abnormality is mutations in the VHL tumour suppressor gene located on the short arm of chromosome 3 (3). Tumors are initiated by biallelic VHL inactivation and are associated with abnormal activation of the hypoxic gene response pathways. The most frequent tumors are retinal and CNS hemangioblastomas, followed by clear cell RCC, pheochromocytoma, pancreatic islet tumors and endolymphatic sac tumors (4). In addition, renal and pancreatic cysts, as well as epididymal or broad ligament cystadenomas also occur. All of the tumors that are typically found in VHL disease can occur as a sporadic event and so a clinical diagnosis of VHL disease in a patient without a positive family history requires the presence of two tumors (e.g., two haemangioblastomas or a haemangioblastomas

and a visceral tumour). Although specific gene mutation can be demonstrated, diagnosis is generally clinical and depends primarily on imaging (2).

In the present case, ^{68}Ga-DOTANOC PET-CT demonstrated both CNS and visceral tumors. Pancreatic tumors occur in 5-10% of cases of VHL and are usually solid non-secretory islet cell tumors. ^{68}Ga-DOTANOC PET-CT is very useful for the diagnosis and staging of pancreatic NET (5). Given the hypervascular nature of both RCC and NET, it could be difficult to differentiate metastatic RCC from pancreatic NET on CECT alone, as was in the present case. The problem became more complex as the pancreatic tumor was non-functioning. In our patient, ^{68}Ga-DOTANOC PET-CT not only characterized the pancreatic mass as NET, it also demonstrated liver metastasis from the pancreatic NET. The left RCC also demonstrated mild ^{68}Ga-DOTANOC uptake, confirming SSTR expression. Therefore, it should be remembered that primary RCC may also express SSTR, especially in cases with high aggressive behaviour (6). However, the clinical and diagnostic value of this observation remains unknown. Although there were no catecholamine producing tumor in the present patient, VHL syndrome is associated with higher risk of such tumors. Risk of pheochromocytoma and paraganglioma in VHL varies according to the clinical subtype and underlying VHL mutation. ^{68}Ga-DOTANOC PET-CT has shown high accuracy for diagnosis and localisation of pheochromocytoma and paraganglioma (7). Therefore, it can be used to localize the lesion if biochemical workups are suggestive of catecholamine secreting tumors.

Central nervous system hemangioblastomas are cardinal feature of VHL syndrome and occur in 60-80% of VHL patients, with cerebellum being the most common site (8). VHL syndrome associated hemangioblastomas frequently expresses SSTR (9). Ambrosini et al. (10) have previously demonstrated *in vivo* SSTR expression in VHL associated hemangioblastoma with ^{68}Ga-DOTANOC PET-CT. In the present case ^{68}Ga-DOTANOC PET-CT detected previously unknown cerebellar hemangioblastoma, which was confirmed on contrast enhanced MRI. Retinal angiomas (hemangioblastoma) are the most common presenting feature of VHL disease as was in the present case, though not recognized at that point of time. ^{68}Ga-DOTANOC PET-CT detected the retinal lesions and were subsequently confirmed with MRI. To our knowledge, there is no previous published report of imaging retinal hemangioblastoma with ^{68}Ga-DOTANOC PET-CT.

We have presented here a classical case of rare VHL syndrome with cerebellar hemangioblastoma, retinal hemangioblastoma, RCC, metastatic pancreatic NET, pancreatic cysts and renal cysts, where ^{68}Ga-DOTANOC PET-CT visualized all of the lesions. In addition, ^{68}Ga-DOTANOC PET-CT also helped in selection of therapy with radiolabelled somatostatin analogue (^{177}Lu-DOTATATE) in this patient. The findings of the present report are the first to highlight the utility of ^{68}Ga-DOTANOC PET-CT based SSTR imaging in VHL syndrome for detecting CNS and visceral malignancies. Further evaluation of role of PET-CT based SSTR imaging in patients with or at risk of VHL syndrome is needed to delineate its role in routine management of such patients, both for diagnosis, as well as for deciding the therapeutic strategy. In our opinion, it should be routinely employed in such patients.

REFERENCES

1. Richard S, Graff J, Lindau J, Resche F. Von Hippel-Lindau disease. *Lancet* 2004;363:1231-1234
2. Fanti S, Ambrosini V, Tomassetti P, Castellucci P, Montini G, Allegri V, et al. Evaluation of unusual neuroendocrine tumours by means of 68Ga-DOTA-NOC PET. *Biomed Pharmacother* 2008;62:667-671
3. Maher ER, Iselius L, Yates JR, Littler M, Benjamin C, Harris R, et al. Von Hippel-Lindau disease: a genetic study. *J Med Genet* 1991;28:443-447
4. Lonser RR, Glenn GM, Walther M, Chew EY, Libutti SK, Linehan WM, et al. von Hippel-Lindau disease. *Lancet* 2003;361:2059-2067
5. Kumar R, Sharma P, Garg P, Karunanithi S, Naswa N, Sharma R, et al. Role of (68)Ga-DOTATOC PET-CT in the diagnosis and staging of pancreatic neuroendocrine tumours. *Eur Radiol* 2011;21:2408-2416
6. Reubi JC, Kvols L. Somatostatin receptors in human renal cell carcinomas. *Cancer Res* 1992;52:6074-6078
7. Naswa N, Sharma P, Nazar AH, Agarwal KK, Kumar R, Ammini AC, et al. Prospective evaluation of ^{68}Ga-DOTA-NOC PET-CT in phaeochromocytoma and paraganglioma: preliminary results from a single centre study. *Eur Radiol* 2012;22:710-719
8. Maher ER, Neumann HP, Richard S. von Hippel-Lindau disease: a clinical and scientific review. *Eur J Hum Genet* 2011;19:617-623
9. Reubi JC, Waser B, Laissue JA, Gebbers JO. Somatostatin and vasoactive intestinal peptide receptors in human mesenchymal tumors: in vitro identification. *Cancer Res* 1996;56:1922-1931
10. Ambrosini V, Campana D, Allegri V, Opocher G, Fanti S. 68Ga-DOTA-NOC PET/CT detects somatostatin receptors expression in von hippel-lindau cerebellar disease. *Clin Nucl Med* 2011;36:64-65